APPLIED AND ENVIRONMENTAL MICROBIOLOGY, Jan. 2005, p. 240–246 Vol. 71, No. 1
0099-2240/05/$08.00+0 doi:10.1128/AEM.71.1.240–246.2005

Quantification of Ammonia-Oxidizing Bacteria and Factors Controlling Nitrification in Salt Marsh Sediments

Sherry L. Dollhopf,[1] Jung-Ho Hyun,[2] April C. Smith,[1] Harold J. Adams,[1] Sean O'Brien,[1] and Joel E. Kostka[1]*

Department of Oceanography, Florida State University, Tallahassee, Florida,[1] and Marine Microbiology Laboratory, Korea Ocean Research and Development Institute, Seoul, Korea[2]

Received 3 May 2004/Accepted 24 August 2004

To elucidate the geomicrobiological factors controlling nitrification in salt marsh sediments, a comprehensive approach involving sediment geochemistry, process rate measurements, and quantification of the genetic potential for nitrification was applied to three contrasting salt marsh habitats: areas colonized by the tall (TS) or short (SS) form of *Spartina alterniflora* and unvegetated creek banks (CBs). Nitrification and denitrification potential rates were strongly correlated with one another and with macrofaunal burrow abundance, indicating that coupled nitrification-denitrification was enhanced by macrofaunal burrowing activity. Ammonia monooxygenase (*amoA*) gene copy numbers were used to estimate the ammonia-oxidizing bacterial population size (5.6×10^4 to 1.3×10^6 g of wet sediment^{-1}), which correlated with nitrification potentials and was 1 order of magnitude higher for TS and CB than for SS. TS and CB sediments also had higher Fe(III) content, higher Fe(III)-to-total reduced sulfur ratios, higher Fe(III) reduction rates, and lower dissolved sulfides than SS sediments. Iron(III) content and reduction rates were positively correlated with nitrification and denitrification potential and *amoA* gene copy number. Laboratory slurry incubations supported field data, confirming that increased amounts of Fe(III) relieved sulfide inhibition of nitrification. We propose that macrofaunal burrowing and high concentrations of Fe(III) stimulate nitrifying bacterial populations, and thus may increase nitrogen removal through coupled nitrification-denitrification in salt marsh sediments.

Nitrogen (N) is most often implicated as the nutrient limiting primary production in the coastal ocean (36), and increased anthropogenic loading may jeopardize important coastal marine ecosystems through eutrophication. Coastal salt marshes may intercept or remove land-derived nutrients along the land-to-sea continuum, thereby regulating coastal primary production (phytoplankton, macroalgae, and sea grasses) and modifying trophic structure (44). Carbon and nutrients are generally considered to be retained and rapidly recycled within marshes (2, 44). However, the physical and biological complexity of the salt marsh environment has made it difficult to predict the factors controlling N cycling processes in marshes, and the mass balance of sources and sinks of N remains uncertain (12, 19).

Nitrification is thought to limit the rate of N removal in many marine sediments (19, 28). Two distinct microbial populations are involved in nitrification: ammonia-oxidizing bacteria (AOB), which catalyze the oxidation of ammonia (NH_3) to nitrite, and nitrite-oxidizing bacteria, which catalyze the oxidation of nitrite to nitrate. Although studies of nitrification rates in salt marsh sediments have found considerable variability across horizontal, vertical, and temporal scales, the environmental factors controlling nitrification rates in salt marsh sediments have not been investigated (3, 42, 43). In other coastal marine sediments, nitrification is influenced by a suite of environmental parameters, including oxygen and dissolved sulfide concentrations, overall rates of C metabolism, and the presence or absence of vegetation and macrofauna (19).

Macrobenthic organisms stimulate microbial metabolism through bioturbation (biologically mediated sediment mixing), which enhances the delivery of substrates and removal of toxic metabolites. For example, sulfate reduction has been considered the dominant microbial respiration process in salt marsh sediments (2); however, recent studies indicate that the Fe cycle can be stimulated by bioturbation in Fe(III)-rich salt marsh sediments, allowing Fe(III) reduction to account for a substantial portion of organic matter oxidation (23, 26). Shifts in microbial respiration pathways may be very important in the regulation of N removal in salt marshes. It is known that macrobenthos can increase nitrification and denitrification rates dramatically in subtidal marine sediments (19, 28), but the effect of macrobenthos on N cycling in intertidal sediments is not well studied.

New methods targeting functional genes that encode for enzymes involved in specific N transformations allow the direct quantification and identification of microorganisms involved in N cycling (35, 48). An example of such a functional gene is *amoA*, which encodes for the first subunit of ammonia monooxygenase, a protein involved in the oxidation of NH_3 to NO_2^-. The *amoA* gene has been used to quantify and characterize AOB in terrestrial and aquatic systems. The results of these studies have increased our knowledge of the diversity, habitats, and activities of this important group of microorganisms (35). Although some 16S rRNA gene-based surveys of AOB in marine sediments have been performed (15, 35, 39), the *amoA* gene in marine sediments has not been studied extensively (9, 14, 31).

* Corresponding author. Mailing address: Department of Oceanography, Florida State University, 317 OSB, Tallahassee, FL 32306-4320. Phone: (850) 645-3334. Fax: (850) 644-2581. E-mail: jkostka@ocean.fsu.edu.

TABLE 1. Ecological and geochemical characteristics of SERF sampling sites[a]

Season and site	Fe(III) (mmol m^{-2})	Fe(III) reduction (mmol m^{-2} day^{-1})	TRS (mmol m^{-2})	HS^- (mmol m^{-2})	Burrows (m^{-2})	AG Bio (g of C m^{-2})	BG Bio (g of C m^{-2})	Fe(III)/TRS
Summer								
TS	2,207	458.0	1,203	0.0040	314	638	1,227	1.8
CB	2,881	104.2	3,845	0.0050	184	0	204	0.75
SS	338	Below detection limit	6,752	11	53	130	5,174	0.05
Winter								
TS	2,767	3.1	7,082	0.0080	352	362	2,316	0.39
CB	3,860	150.2	6,119	0.0080	58	0	191	0.63
SS	1,249	Not done	5,624	0.0090	99	51	6,611	0.22

[a] Geochemical constituents are calculated as the average total sediment inventory ($n = 6$) integrated to a 6-cm depth. TRS, total reducible sulfur; HS^-, soluble hydrogen sulfide; AG Bio, aboveground biomass; BG Bio, belowground biomass.

In this study, our goal was to elucidate the factors controlling ammonia-oxidizing bacterial abundance and activity in salt marsh sediments. We hypothesized that (i) the metabolic and genetic nitrification potential would be higher in more heavily bioturbated and vegetated salt marsh sediments, and (ii) the presence of reactive Fe(III) minerals would enhance nitrification by protecting AOB from sulfide poisoning. These hypotheses were addressed in the field and in the laboratory through sediment geochemistry, nitrification and denitrification potential rate measurements, and *amoA* gene copy number quantification. A range of salt marsh environments, which varied in their physicochemical characteristics, vegetation coverage, and macrofaunal abundance, were studied. The effects of Fe(III) and sulfide on nitrification were further studied through the manipulation of sediment chemistry in laboratory slurry incubations.

MATERIALS AND METHODS

Sampling area. This study was conducted at the Saltmarsh Ecosystem Research Facility (SERF) adjacent to the Skidaway Institute of Oceanography on Skidaway Island in Savannah, Ga. At SERF, the marsh is dominated by a nearly monospecific stand of the smooth cordgrass *Spartina alterniflora*. The mud fiddler crab *Uca pugnax* is the most abundant bioturbating macroinvertebrate. Sediments were sampled according to a random sampling design at three marsh sites that differed in the abundance of fiddler crab burrows, vegetation coverage, and hydrology (see Table 1). These sites will be referred to as the creek bank (CB), tall *Spartina* (TS), and short *Spartina* (SS) sites. Further information on the sampling area, including sediment characteristics and macrobenthic ecology, can be found in a study by Kostka et al. (23).

Summer and winter sampling dates for all analyses were 21 to 23 July 2002 and 25 to 26 February 2003, with the exception of sediment for the summer nitrification and denitrification potentials, which was collected on 9 September 2002. Samples were collected at random from 12 17- by 17-m grids established at each site during low tide. Sediment temperature ranged from 27 to 31°C during the summer and 10 to 15°C during the winter. Six grids at each site were sampled for geochemical and ecological measurements. Sediment for Fe(III) reduction incubations, nitrification and denitrification potentials, and *amoA* competitive PCR (cPCR) was sampled from one grid at each site.

Ecological measurements. *Uca* burrows and *Spartina* shoots were counted in randomly placed 25- by 25-cm quadrants in each grid that was chosen for sediment sampling. Above- and belowground plant biomass was determined by collecting large cores (internal diameter, 8 cm) in each site described. Aboveground shoots were severed from the core at the sediment surface. Belowground biomass, to a depth of 25 cm, was sieved to remove excess sediment from the core. Biomass was then rinsed and dried to a constant weight at 60°C. Ash weights were obtained to determine the percentage of organic carbon by measuring loss on ignition at 550°C for 6 h. Statistical analyses were performed by using GraphPad Prism version 4.00 for Windows (GraphPad Software, San Diego, Calif.). Spearman correlation values were calculated due to the nonparametric nature of the data. Both ecological and geochemical data were separated into 0- to 3- and 3- to 6-cm depth intervals, resulting in 12 separate data points for all statistical tests.

Pore water geochemistry. Sediments were sampled by driving a polycarbonate core liner (internal diameter, 6 cm) at least 10 cm deep into the sediment. All extraction and processing of pore waters was conducted under strictly anoxic conditions in a N_2-filled glove bag. The cores were stored on ice for 3 h or less and sectioned into 0- to 3- and 3- to 6-cm depth intervals. The sediment from each section was placed into a polypropylene centrifuge tube and tightly capped. After centrifugation at 5,000 × *g* for 20 min, the supernatant was collected, filtered through 0.2-μm-pore-size cellulose acetate syringe filters, and fixed with Zn or HCl. Fixed pore waters were frozen immediately after fixation until analysis. Dissolved sulfide was determined in pore waters fixed in Zn by using the methylene blue method (detection limit, 1 μM; standard deviation, 5%) (11). Dissolved Fe^{2+} was determined in pore waters fixed in HCl (0.1 N) by colorimetry with a ferrozine solution (detection limit, 1 μmol $liter^{-1}$; standard deviation, 2%) (40). Pore water [NO_x] was determined by chemiluminescence after reduction to NO (8).

Solid-phase geochemistry. Cut-off 60-ml syringe barrels were used to sample sediments to a depth of 10 cm. These cores were immediately sealed with butyl rubber stoppers and electrical tape and stored on ice. Within 3 h, they were frozen at −20°C until further analysis. Wet chemical extractions were used to determine the concentration of poorly crystalline Fe(III) oxide minerals in 1-cm intervals down to a 6-cm depth. Total Fe was extracted from air-dried sediment in 0.2 mol of oxalate $liter^{-1}$ (pH 3) for 4 h, and Fe(II) was similarly extracted from fresh frozen sediment in anoxic oxalate (41). Oxalate-extractable Fe(III) was defined as the difference between these two measures. Calibration experiments with pure Fe phases have confirmed the selectivity of this extraction towards poorly crystalline Fe phases (24). Total reducible sulfur (TRS), which included both acid-volatile sulfide ($FeS + H_2S$) and chromium-reducible sulfur ($S^0 + FeS_2$), was determined after a single-step distillation with cold 2 N HCl and boiling 0.5 M Cr^{2+} solution (13).

Iron reduction rates. Sediment samples were collected from 0- to 3- and 3- to 6-cm depth intervals with a trowel into 1-gallon Ziploc bags and stored on ice until analysis. Within 3 h of sampling, the sediments were homogenized and loaded into 50-ml polypropylene centrifuge tubes in an N_2-filled glove bag. Sediments were incubated at in situ temperature in the dark, and duplicate tubes were sampled at regular intervals as described previously by Kostka et al. (23). Iron was extracted and speciated at each time point by using oxalate as described above. The Fe(III) reduction rate was determined by regression of the accumulation of Fe(II) with time. The residence time at each depth interval was calculated by dividing the total reactive Fe(III) found in a depth interval by the Fe(II) accumulation rate in the corresponding sediment incubation.

Nitrification potential rate measurements. The homogenized sediment samples used for Fe(III) reduction incubations were also used for nitrification and denitrification potential measurements and for quantification of the *amoA* gene. Samples from each depth were slurried (5.0 g of wet sediment + 50 ml of sterile artificial seawater) and placed into 250-ml Erlenmeyer flasks. Duplicate flasks from each site were amended with ammonium (NH_4SO_4; 500 μmol $liter^{-1}$) and sodium chlorate (10 mmol $liter^{-1}$). Control flasks contained ammonium, sodium chlorate, and allylthiourea (ATU; 20 mg $liter^{-1}$) (4). Flasks were capped with aluminum foil and incubated in the dark at 25°C with constant shaking (150 rpm). Samples were collected at intervals between 0 and 24 h. Potential nitrification rates (linear regression of the increase in [NO_x] [$NO_3^- + NO_2^-$] over time) for all treatments were calculated after subtracting the increase in [NO_x] in

the ATU control flasks. [NO_x] was determined in interstitial waters of the slurry samples as described above. Nitrite concentrations were determined spectrophotometrically in random samples (16) and were within 5 μmol liter^{-1} of [NO_x] concentrations at all time points.

Denitrification potential rate measurements. The acetylene block technique was used to determine potential denitrification rates (38). Twenty grams of wet sediment from each site, 50 ml of artificial seawater, and 100 μmol of KNO_3 liter^{-1} was added to duplicate 200-ml serum bottles and sealed with a stopper and crimp cap. The headspace of each bottle was flushed with N_2 for 10 min prior to the addition of 10 ml of acetylene. After a 1-h incubation at 25°C, 20 ml of headspace was sampled and injected into 20-ml Vacutainers. Gas samples were stored at −20°C before quantification of N_2O production by using a Shimadzu gas chromatograph with an electron capture detector. In parallel control experiments, further degassing and the addition of Fe(III) to remove sulfides did not substantially change the denitrification rate measurements. Time course experiments, including duplicate treatments for all sites, indicated that potential denitrification rates declined after the first hour of incubation; thus, 1-h incubations were used.

Quantification of the *amoA* gene copy number. The number of *amoA* gene copies per gram of sediment was determined with the *amoA* cPCR assay as described by Bjerrum et al. (5), except that DNA was extracted from 0.25 g of wet sediment with a Mo Bio UltraClean soil DNA extraction kit (Solana Beach, Calif.). Each sample was extracted in duplicate. Two separate cPCR assays were performed on each extract by using 1.0- or 0.5-μl aliquots of environmental DNA in each reaction, resulting in four cPCR assays for each sediment sample. Competitor dilution series for all assays consisted of 1,000, 500, 100, 50, 10, and 0 competitor molecules. In samples with high *amoA* copy numbers, the assay was repeated with an extra reaction containing 5,000 competitor molecules for increased accuracy. Amplification efficiency was tested by spiking sediment extracts with 1,000 copies of the *amoA* gene. Overall efficiency (extraction plus amplification) was tested by spiking sediment from the 0- to 3-cm depth interval sediment of each site (0.25 g [wet weight]) with 10^5 copies of the *amoA* gene. The *amoA* gene from *Nitrosomonas europea* cloned into plasmid pCR2.1 (Invitrogen) was used for spiking cPCR reactions, positive controls, and template competitor construction.

Laboratory inhibition of nitrification. To determine the effect of sulfide and ferrihydrite (FeOOH) on potential nitrification rates, duplicate flasks containing 1.0 g of wet TS sediment and 50 ml of sterile artificial seawater were amended with 500 μmol of NH_3 liter^{-1} and 10 mmol of sodium chlorate liter^{-1} and treated with either no additional amendment, 1.0 mmol of sulfide liter^{-1}, 2 mmol of FeOOH liter^{-1}, or 1.0 mmol of sulfide liter^{-1} and 2 mmol of synthetic FeOOH liter^{-1}. Control flasks for each treatment contained 20 mg of ATU liter^{-1}. The pH in all flasks was adjusted to 7.8 (4). Synthetic FeOOH was prepared according to the method described by Kostka and Nealson (25). In a separate experiment, duplicate sterile flasks received 1, 2, or 5 g of wet sediment from the TS site (0- to 3-cm depth) plus 50 ml of sterile artificial seawater, 500 μM NH_3, and 10 mM sodium chlorate. One flask for each treatment received 1 mmol of sulfide liter^{-1}, while the other served as a no-sulfide control to correct for any rate differences caused by different sediment/water ratios. The pH was adjusted to 7.8 in all flasks. Stimulation of potential nitrification rates in SS sediment (0- to 3-cm depth) was attempted by oxidizing the sediment prior to incubation by vigorous shaking (200 rpm) for 1 h before adding amendments at time zero.

RESULTS

Macroecological measurements. During summer and winter at the TS site, three to six times as many burrows were observed in comparison to the SS site (Table 1). Seasonal changes in burrow density included a decrease at CB and an increase at TS and SS from summer to winter. Aboveground plant biomass was highest at TS during both summer and winter, while belowground plant biomass was highest at SS (Table 1). At CB, low belowground plant biomass was observed in both seasons, most likely representing detritus, as no live roots were observed. During the winter, aboveground biomass decreased and belowground biomass increased at TS and SS, indicating a reallocation of plant resources to root biomass during the winter.

Sediment geochemistry and iron turnover. Pore water geochemistry, solid-phase geochemistry, and rate measurements revealed dramatic differences between the sites (Table 1). The inventories of geochemical constituents remained within a factor of 2 or 3 for TS and CB, while SS often showed very different geochemistry. Differences were most pronounced during the summer, when Fe(III) inventories were more than seven times larger and TRS inventories were two to three times smaller at TS and CB than at SS (Table 1). Dissolved sulfide inventories for SS were several orders of magnitude higher than for TS and CB during the summer. Iron(III) inventories increased, and no dissolved sulfide accumulated at all sites during the winter. TRS inventories at TS and CB also increased in the winter. A further indication of the redox poise of the sediments can be found in the ratio of Fe(III) to TRS (Table 1). At SS, the Fe(III)/TRS ratio remained at <0.3, whereas the ratio was always >0.4 at TS and CB.

In accordance with the low Fe(III) content of SS sediments, no Fe(III) reduction was detected at SS during the summer, while TS and CB sediments exhibited rapid Fe(III) reduction rates and the short Fe(III) residence times of 10 and 55 days, respectively (Table 1). Winter Fe(III) reduction rates were three times higher than summer rates at CB, which decreased the residence time of Fe(III) to 26 days despite the increase in CB Fe(III) inventory. TS sediments exhibited lower winter Fe(III) reduction rates, resulting in a Fe(III) residence time of almost 900 days. SS sediment was not tested for Fe(III) reduction in the winter.

Nitrification potential. Nitrification potential was 10 times higher in TS than in SS sediment, regardless of sediment depth or season, while CB nitrification potentials were at intermediate levels between the two (Fig. 1A). Seasonal differences in depth-integrated potential rates were also apparent. At TS, depth-integrated potential rates (0 to 6 cm) were higher during the summer (1,486 μmol of N m^{-2} h^{-1}) than in the winter (1,057 μmol of N m^{-2} h^{-1}). Depth-integrated summer potential rates at SS were small (129 μmol of N m^{-2} h^{-1}), but were higher than winter potential rates, which were slightly negative (−51 μmol of N m^{-2} h^{-1}). In CB sediments, depth-integrated potential rates were similar during the summer (628 μmol of N m^{-2} h^{-1}) and winter (620 μmol N m^{-2} h^{-1}), indicating that the size of the nitrifying bacterial population was similar in the two seasons.

Significant differences were also observed between the 0- to 3- and 3- to 6-cm sediment depth intervals at TS and CB (Fig. 1A). During the summer, nitrification potential was highest in the 0- to 3-cm depth interval at both sites, whereas during the winter, nitrification potential was highest in the 3- to 6-cm depth interval at both sites. A shift of nitrifying activity deeper into the sediment was also supported by TS NO_3^- depth profiles, which showed a shift of maximum pore water NO_3^- concentrations from a ~2-cm depth in the summer to a ~4-cm depth in the winter (J. E. Kostka, unpublished data).

Denitrification potential. Similar to nitrification potentials, denitrification potential rates were, on average, an order of magnitude higher in TS than SS sediments, while CB denitrification potentials were generally at intermediate levels between the two (Fig. 1B). At TS and CB, depth-integrated rates (0 to 6 cm) were higher in the summer (4,375 and 3,517 μmol of N m^{-2} h^{-1}, respectively, for TS and CB) than in the winter

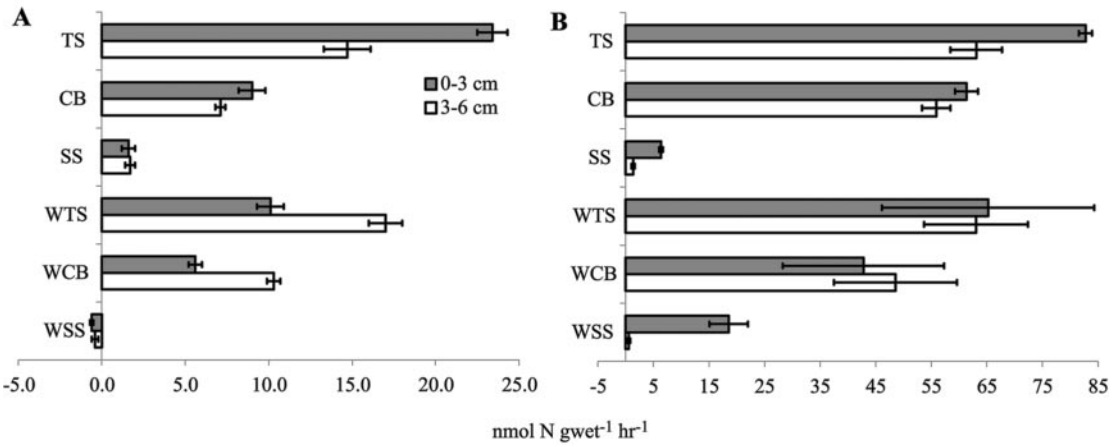

FIG. 1. Nitrification potential (A) and denitrification potential (B) rates in SERF sediments during summer and winter as determined with sediment slurries. Winter samples have a W prefix. Error bars represent the standard error of the rate calculated from linear regression of duplicate assays. gwet, grams (wet weight).

(3,848 and 2,741 μmol of N m^{-2} h^{-1}, respectively, for TS and CB), while winter rates were higher in SS sediments (574 versus 232 μmol of N m^{-2} h^{-1}, respectively, for winter versus summer). Winter CB sediments were the only sediments to show a higher denitrification potential in the 3- to 6-cm depth interval than in the 0- to 3-cm interval. Denitrification potential rates were on average three to five times higher than nitrification potentials from the same depth and season.

***amoA* gene copy number.** Copy numbers of the *amoA* gene were 1 to 2 orders of magnitude higher in TS than in SS sediments at all seasons and depths (Table 2). In SS sediments during the summer and at the 3- to 6-cm depth interval during the winter, the number of *amoA* genes per gram of sediment was actually below the detection limit of our assay (10^3 copies g [wet weight]$^{-1}$). TS also had consistently higher *amoA* gene copy numbers than CB; however, these differences were not statistically significant. Seasonal changes in *amoA* copy number were not as apparent as changes in nitrification potentials, as no significant decrease in copy number was observed during the winter. The only noticeable change in the winter samples was an increase in *amoA* gene copy numbers in the CB at the 3- to 6-cm depth interval and at SS at the 0- to 3-cm depth interval. The observed increases were accompanied by an increase in variability between samples, as indicated by the larger standard errors in Table 2.

SS sediments spiked with a known number of *amoA* gene copies yielded an overall extraction and amplification efficiency of 14%, similar to those of TS and CB sediments (efficiencies of 16 and 12%, respectively), indicating that the differences in estimated copy number were not due to different sediment characteristics affecting the extraction and amplification of nucleic acids. The efficiency of the cPCR assay was similar to that of other quantitative PCR assays applied to sediments, and may be related to the high organic matter and clay content, which are known to interfere with DNA extraction, purification, and PCR amplification (27, 34).

Inhibition of nitrification. We tested whether increasing amounts of reactive Fe(III) could prevent sulfide inhibition of nitrification by adding either synthetic FeOOH or different amounts of Fe(III)-rich TS sediment to nitrification potential rate assays (Table 3). The addition of 2 mmol of synthetic FeOOH liter^{-1} to slurries containing 1 g of wet sediment decreased sulfide inhibition dramatically, from 96 to only 40% (Table 3). The addition of FeOOH alone had no effect on nitrification potential. In a 1-g wet sediment slurry containing 1 mmol of sulfide liter^{-1}, nitrification was inhibited by 75%

TABLE 2. *amo*A gene copy number in SERF sediments during summer and winter determined by cPCR[a]

Site	Depth (cm)	*amo*A copies (g [wet wt]$^{-1}$ × 10^5) in:	
		Summer	Winter
TS	0 to 3	2.1 ± 0.76	2.5 ± 1.4
	3 to 6	1.6 ± 0.73	1.2 ± 0.47
CB	0 to 3	0.73 ± 0.20	0.40 ± 0.078
	3 to 6	0.59 ± 0.21	4.4 ± 3.5
SS	0 to 3	<0.1	0.19 ± 0.13
	3 to 6	<0.1	<0.1

[a] Values shown are raw determinations not corrected for cPCR efficiency plus or minus 1 standard deviation.

TABLE 3. Sulfide inhibition of nitrification rates in the presence of synthetic FeOOH or Fe(III)-rich TS sediment in sediment slurries[a]

Treatment	nmol of NO_x h^{-1} g of wet sediment^{-1}
Unamended	16.5 ± 1.3
FeOOH	18.5 ± 2.1
FeOOH + sulfide	9.9 ± 1.7
Sulfide	0.7 ± 1.3
1 g of wet sediment	23.7 ± 3.0
1 g of wet sediment + sulfide	5.9 ± 1.3
2 g of wet sediment + sulfide	11.8 ± 2.8
5 g of wet sediment + sulfide	20.9 ± 1.9

[a] Rates were calculated by linear regression of NO_x production in duplicate flasks for each treatment.

compared to an analogous slurry without sulfide. Slurries containing 2 or 5 g of wet sediment plus 1 mmol of sulfide liter^{-1} were inhibited by only 56 and 28%, respectively, compared to identical slurries without sulfide. The rate of nitrification per gram of sediment in the slurries without sulfide varied by less than 8% between the different sediment amounts, indicating a negligible effect of sediment dilution. The addition of FeOOH and sulfide alone or together had no impact on potential nitrification rates in SS sediment, which were negligible for all treatments (data not shown).

DISCUSSION

AOB abundance. Determination of *amoA* gene copy number by competitive PCR provides a measure of the genetic potential for nitrification without prior cultivation or sediment manipulation. *amoA* gene copy numbers showed a strong positive correlation with nitrification potentials in our study ($P = 0.0007$; $r = 0.838$), thereby providing a cultivation-independent validation for the use of nitrification potential rate measurements to estimate AOB population size (Fig. 1 and Table 2). When the *amoA* gene copies per gram of wet sediment are corrected for the overall efficiency of the cPCR assay, we calculate 1.4×10^5 to 3.2×10^6 of *amoA* gene copies g (wet weight)$^{-1}$ in salt marsh sediments with detectable levels of the *amoA* gene. Considering an average of 2.5 copies of the *amoA* gene in the genome of ammonia-oxidizing bacteria in the β subdivision of the class *Proteobacteria* (β-*Proteobacteria*) (32), we estimate an abundance of 5.6×10^4 to 1.3×10^6 of AOB g (wet weight)$^{-1}$ salt marsh sediment. Our AOB population estimates overlap with the ranges determined for flooded rice paddy soils (10^3 to 10^5 cells g [wet weight]$^{-1}$) and riverine sediment (10^5 to 10^7 cells g^{-1}) by using *amoA* or 16S rRNA gene-based cPCR assays (5, 34).

Cell-specific ammonium oxidation rates in the nitrification potential assays calculated by using estimated AOB abundances range from 0.004 to 0.018 fmol of NH_3 cell^{-1} h^{-1}. This range is 2 to 3 orders of magnitude lower than the cellular oxidation rates calculated for nitrifying bacteria in pure cultures and in soil (33). It might be expected that cellular ammonium oxidation rates in potential assays would be closer to pure culture values, given that ammonium oxidation should not be limited by either oxygen or ammonium. In situ cellular oxidation rates would most likely be lower than those calculated for potential nitrification assays due to oxygen limitation. Molecular characterization of marine sediment AOB communities suggests that the dominant AOB in marine sediments are not represented in pure culture (9, 14, 31). Thus, the low cellular oxidation rates may indicate that marine sediment AOB have very different growth kinetics than the AOB currently in culture.

Molecular oxygen is depleted within the top few millimeters of the sediment surface and burrow walls in the SERF marsh (15a). Thus, the observation of significant AOB populations in anoxic SERF sediments suggests that either aerobic nitrification is supported by an ephemeral oxygen supply or anoxic nitrification may be occurring. Although AOB (e.g., *Nitrosomonas* species) are capable of oxidizing NH_3 via reduction of NO_2^- or N_2O under anaerobic conditions in pure culture (6, 37), we believe that the AOB populations in SERF sediments utilize oxygen supplied by *Spartina* roots and macrofaunal burrows. Other studies have found that AOB in anoxic sediments are associated with plant roots and macrofaunal burrows, suggesting that the bacteria utilize O_2 transported into the sediment by macrobenthic activities (7, 18). We also found a significant correlation between burrow abundance and *amoA* gene copy number. In addition, aerobic nitrification activity began without a lag phase in the nitrification potential assays (Table 3), suggesting that sediment AOB were active and expressing aerobic nitrification genes. Anaerobic NH_3 oxidation in these sediments cannot be ruled out, however, and more study is needed to determine if it is important to N cycling in salt marsh sediments.

Although our findings agree with those of previous studies, it should be noted that in this study and others, the *amoA* primers used are specific for ammonia-oxidizing β-*Proteobacteria*. Therefore, our AOB population estimates do not account for all phylogenetic groups capable of ammonia oxidation, such as the γ-*Proteobacteria* or other unknown AOB that may be present in these sediments. However, primers targeting γ-*Proteobacteria amoA* genes never yielded amplification products in SERF sediments (data not shown), and previous studies have failed to detect γ-*Proteobacteria amoA* genes in other marine sediments (15, 31).

Effects of macroorganisms. The stimulatory effects of bioturbation by macrobenthic organisms on both nitrification and denitrification in subtidal sediments have been well documented (1, 28). One consequence of bioturbation that stimulates nitrification is the expansion of the oxic-anoxic interface where conditions for AOB are favorable. The increase in this contact zone can increase the volume of oxidized sediment by 30 to 50% (29). Both experimental and modeling data indicate that the stimulation of nitrification by increased O_2 penetration into the sediment enhances denitrification as well (1). Using burrow density as an indicator of bioturbation activity, we found that nitrification potential, *amoA* gene copy number, and denitrification potential were all positively correlated with bioturbation ($P = 0.018$, 0.029, and 0.007; $r = 0.6643$, 0.6263, and 0.834, respectively). In support of our observations, radial coring of fiddler crab burrows at SERF clearly showed that sediments and pore waters in a 2-cm radius around each burrow are significantly more oxidized than bulk sediment (17) . Microbial Fe(III) reduction rates were also significantly higher near burrow walls than in bulk sediment (17).

Past studies have indicated that vegetated sediments support nitrification and denitrification rates 4 to 20 times greater than unvegetated sediments in subtidal marine environments through the enhanced transport of O_2 and carbon substrates (10). However, we observed insignificant correlation coefficients between plant biomass and nitrification activity.

Nitrification and denitrification potential in salt marsh sediments. In contrast to the abundance of nitrification measurements carried out in subtidal marine environments (18, 19, 20), few nitrification rates have been determined in salt marsh sediments. The range of potential rates we report here (0 to 23 nmol of N g [wet weight]$^{-1}$ h^{-1}) is slightly lower than the range observed in subtidal sediments (0 to 50 nmol of N g [wet weight]$^{-1}$ h^{-1}) (18). In three previous studies, nitrification rates in salt marsh sediments were similar to the lowest rates we measured at SS and 10 to 40 times lower than the rates we observed at TS (see summary in Table 4). The majority of sites

TABLE 4. Nitrification and denitrification rates in saltmarsh sediments

Vegetation	Nitrification (μmol of N m^{-2} h^{-1})	Denitrification (μmol of N m^{-2} h^{-1})	Reference
CB, SS, TS	−23 to 913	195 to 3,228	This study
Not described	0 to 29	21 to 63	Thompson et al. (42)
CB, SS	0 to 79	0 to 2	Anderson et al. (3)
SS	2 to 25	0 to 340	Tobias et al. (43)
CB, SS, pannes		71 to 214	Kaplan et al. (22)
Mudflat		1 to 115	Koch et al. (22a)
Not described		−41 to 834	Johnson et al.
SS		75	White and Howes (47)
Not described		65 to 1,820	Lee et al. (30)

sampled previously were colonized either by short-form *S. alterniflora* or were not well described in relation to vegetation and macrobenthos.

More denitrification rate measurements than nitrification rate measurements have been made in salt marsh sediments (Table 4). Our potential rate measurements overlap with the range of potentials reported by Lee et al. (30) using similar methods in various New England salt marshes. The range of denitrification potentials that we measured at SS (195 to 585 μmol of N m^{-2} day^{-1}) are within a factor of 2 or 3 of the rate measurements made at *S. alterniflora*-colonized sites in the Great Sippewissett marsh (22, 47), although the Great Sippewissett measurements were made by using an intact core method (Table 4). Approximately one-third of the area of the SERF and Great Sippewissett marshes is vegetated by short-form *S. alterniflora*, with the remainder comprised of creek bank and tall-form *S. alterniflora* habitats (23, 45). Considering that our results show that denitrification is roughly 10 times higher at TS and CB (range, 1,614 to 3,228 μmol of N m^{-2} day^{-1}) than at SS, we suggest that the importance of denitrification in salt marsh ecosystem N budgets may have been underestimated in past studies, which have sampled marsh sediments vegetated mainly by short-form *S. alterniflora*.

We observed a strong positive correlation ($P = 0.0003$; $r = 0.8671$) between nitrification and denitrification potentials that is in agreement with numerous other studies indicating that denitrification and nitrification are tightly coupled when external supplies of nitrate are low (19, 20), as they are in this Georgia salt marsh (46). Denitrification potentials were, on average, a factor of 2 higher than nitrification potentials measured in the same sediments (Fig. 1). This result may be explained by the metabolic versatility and fast maximum growth rates of denitrifiers in comparison to nitrifiers (48).

Effect of sulfide and Fe(III) on nitrification. Very little information is available about the linkages between dissolved sulfide concentrations, Fe(III) minerals, and microbial N transformations in marine sediments. We observed positive correlations between independent measures of N cycling (nitrification potential, *amoA* gene copy number, and denitrification potential) and Fe(III) reduction rates ($P = 0.005$, 0.008, and 0.0118; $r = 0.7537$, 0.7195, and 0.6966, respectively), suggesting that the Fe and N cycles may interact in salt marsh sediments (Fig. 2). Previous studies of Georgia salt marshes have shown that sites similar to TS consistently support extremely high rates of SO_4^{-2} reduction (17, 23, 26), and SO_4^{-2} reduction rates measured concurrently with the present study support

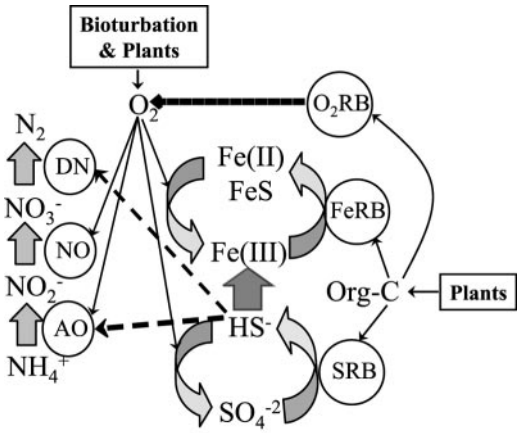

FIG. 2. Conceptual model illustrating the effect of bioturbation and plants on interactions between the Fe, N, and S cycles. FeRB, Fe(III)-reducing bacteria; SRB, sulfate-reducing bacteria; O_2RB, oxygen-reducing bacteria; AO, ammonia oxidizers; NO, nitrite oxidizers; DN, denitrifiers; Org-C, organic carbon; solid black lines, positive effects; broken black lines, negative effects.

this trend (J. H. Hyun, unpublished data) The increased potential for nitrification and denitrification at TS is therefore not related to a decrease in the rate of sulfide production from SO_4^{-2}. Reactive Fe(III) compounds react rapidly with sulfides, thereby scavenging sulfides formed through SO_4^{-2} reduction (Fig. 2). These reactions exert a very important control on the distribution of sulfide in marine systems (41). The presence of a large reactive iron pool that is rapidly recycled may thereby protect nitrifying bacteria from sulfide inhibition.

Results from our lab slurry incubations support the field data and indicate that increased amounts of reactive Fe(III) relieve sulfide inhibition (Table 3). Joye and Hollibaugh (21) investigated the effect of Fe(III) on sulfide inhibition by exposing sediment slurries to sulfide and then adding Fe(III) in the form of goethite. The goethite addition had no effect on nitrification rates. We found that both synthetic ferrihydrite (FeOOH) and natural Fe(III) compounds protected nitrifying bacteria from sulfide inhibition if the Fe(III) was added before the sulfide (Table 3). Exposing nitrifying bacteria to sulfide prior to adding oxidized iron may allow sulfides to bind to ammonia monooxygenase, irreversibly inhibiting this key nitrification enzyme. Because of the speed with which Fe(III) and sulfide react in natural Fe(III)-rich sediments, dissolved sulfide does not accumulate; thus, exposing nitrifying bacteria to high concentrations of sulfide prior to adding Fe(III) does not mimic in situ conditions.

Bioturbation is an important driving factor in the N, Fe, and S cycles of the salt marsh, facilitating solute transport and continually recycling electron acceptors critical to both the oxidation of organic matter and coupled nitrification-denitrification (17, 23, 28) (Fig. 2). Plants may inject oxygen into reduced sediments; however, roots also exude carbon-containing compounds, increasing respiration and oxygen consumption. Iron(III) content and turnover may amplify the positive effects of bioturbation and plants on coupled nitrification-denitrification by binding sulfides before they come in contact with O_2 (Fig. 2). By effectively separating the zone of O_2 penetration from the zone of sulfide accumulation, the zone of Fe(III) reduction may provide a buffer

which allows coupled nitrification-denitrification to occur in sediments with very high rates of SO_4^{-2} reduction.

ACKNOWLEDGMENTS

We thank Mike Dollhopf and Lainie Petrie for expert assistance in sample collection and pore water analysis. We also thank the faculty, staff, and students of the Skidaway Institute of Oceanography, especially Marc Frischer, for allowing us to use their laboratory space and facilities.

This research was funded by a National Science Foundation Postdoctoral Fellowship in Microbial Biology awarded to S.L.D.

REFERENCES

1. **Aller, R. C.** 1988. Benthic fauna and biogeochemical processes in marine sediments: the role of burrow structures, p. 301–338. *In* T. H. Blackburn and J. Sorensen (ed.), Nitrogen cycling in coastal marine environments, vol. 33. John Wiley & Sons, New York, N.Y.
2. **Alongi, D. M.** 1998. Coastal ecosystem processes, p. 43–92. CRC Press, Boca Raton, Fla.
3. **Anderson, I. C., C. R. Tobias, B. B. Neikirk, and R. L. Wetzel.** 1997. Development of a process-based nitrogen mass balance model for a Virginia (USA) *Spartina alterniflora* salt marsh: implications for net DIN flux. Mar. Ecol. Prog. Ser. **159:**13–27.
4. **Belser, L. W., and E. L. Mays.** 1980. Specific inhibition of nitrite oxidation by chlorate and its use in assessing nitrification in soils and sediments. Appl. Environ. Microbiol. **39:**505–510.
5. **Bjerrum, L., T. Kjaer, and N. B. Ramsing.** 2002. Enumerating ammonia-oxidizing bacteria in environmental samples using competitive PCR. J. Microbiol. Methods **51:**227–239.
6. **Bock, E., I. Schmidt, R. Stuven, and D. Zart.** 1995. Nitrogen loss caused by denitrifying *Nitrosomonas* cells using ammonium or hydrogen as electron donors and nitrite as electron acceptor. Arch. Microbiol. **163:**16–20.
7. **Bodelier, P. L. E., J. A. Libochant, C. W. P. M. Blom, and H. J. Laanbroek.** 1996. Dynamics of nitrification and denitrification in root-oxygenated sediments and adaptation of ammonia-oxidizing bacteria to low-oxygen or anoxic habitats. Appl. Environ. Microbiol. **62:**4100–4107.
8. **Braman, R. S., and S. A. Hendrix.** 1989. Nanogram nitrite and nitrate determination in environmental and biological materials by vanadium(III) reduction with chemiluminescence detection. Anal. Chem. **61:**2715–2718.
9. **Caffrey, J. M., N. Harrington, I. Solem, and B. B. Ward.** 2003. Biogeochemical processes in a small California estuary. 2. Nitrification activity, community structure and role in nitrogen budgets. Mar. Ecol. Prog. Ser. **248:**27–40.
10. **Caffrey, J. M., and W. M. Kemp.** 1992. Influence of the submersed plant, Potamogeton perfoliatus, on nitrogen cycling in estuarine sediments. Limnol. Oceanogr. **37:**1483–1495.
11. **Cline, J. D.** 1969. Spectrophotometric determination of hydrogen sulfide in natural waters. Limnol. Oceanogr. **14:**454–458.
12. **Cornwell, J. C., W. M. Kemp, and T. M. Kana.** 1999. Denitrification in coastal ecosystems: methods, environmental controls, and ecosystem level controls, a review. Aquat. Ecol. **33:**41–54.
13. **Fossing, H., and B. B. Jorgensen.** 1989. Measurement of bacterial sulfate reduction in sediments: evaluation of single-step chromium reduction methods. Biogeochemistry **8:**223–245.
14. **Francis, C. A., G. D. O'Mullan, and B. B. Ward.** 2003. Diversity of ammonia monooxygenase (*amoA*) genes across environmental gradients in Chesapeake Bay sediments. Geobiology **1:**129–140.
15. **Freitag, T. E., and J. I. Prosser.** 2003. Community structure of ammonia-oxidizing bacteria within anoxic marine sediments. Appl. Environ. Microbiol. **69:**1359–1371.

15a. **Furukawa, Y., A. C. Smith, J. E. Kostka, J. Watkins, and C. R. Alexander.** 2004. Quantification of macrobenthic impacts on diagenesis using a multicomponent inverse model in saltmarsh sediments. Limnol. Oceanogr. **49:** 2058–2072.

16. **Grasshoff, K.** 1983. Determination of nitrite, p. 139–142. *In* K. Grasshoff, M. Ehrhardt, and K. Kremling (ed.), Methods of seawater analysis, 2nd ed. Verlag Chemie, Weinheim, Germany.
17. **Gribsholt, B., J. E. Kostka, and E. Kristensen.** 2003. Impact of fiddler crabs and plant roots on sediment biogeochemistry in a Georgia saltmarsh. Mar. Ecol. Prog. Ser. **259:**237–251.
18. **Henriksen, K., and W. M. Kemp.** 1988. Nitrification in estuarine and coastal marine sediments, p. 207–249. *In* T. H. Blackburn and J. Sorensen (ed.), Nitrogen cycling in coastal marine environments, vol. 33. John Wiley & Sons, New York, N.Y.
19. **Herbert, R. A.** 1999. Nitrogen cycling in coastal marine ecosystems. FEMS Microbiol. Rev. **23:**563–590.
20. **Jenkins, M. C., and W. M. Kemp.** 1984. The coupling of nitrification and denitrification in two estuarine sediments. Limnol. Oceanogr. **29:**609–619.

20a. **Johnson, R., M. LaMontagne, and I. Valiela.** 1994. Rate of denitrification in submerged salt marsh sediments. Biol . Bull . **187:**289–290.

21. **Joye, S. B., and J. T. Hollibaugh.** 1995. Influence of sulfide inhibition of nitrification on nitrogen regeneration in sediments. Science **270:**623–625.
22. **Kaplan, W., I. Valiela, and J. M. Teal.** 1979. Denitrification in a salt marsh ecosystem. Limnol. Oceanogr. **24:**726–734.

22a. **Koch, M. S., E. Maltby, G. A. Oliver, and S. A. Baker.** 1992. Factors controlling denitrification rates of tidal mudflats and fringing saltmarshes in Southwest England. Estuar. Coast. Shelf Sci. **34:**471–485

23. **Kostka, J. E., B. Gribsholt, E. Petrie, D. Dalton, H. Skelton, and E. Kristensen.** 2002. The rates and pathways of carbon oxidation in bioturbated saltmarsh sediments. Limnol. Oceanogr. **47:**230–240.
24. **Kostka, J. E., and G. W. Luther.** 1994. Partitioning and speciation of solid phase iron in saltmarsh sediments. Geochim. Cosmochim. Acta **58:**1701–1710.
25. **Kostka, J. E., and K. H. Nealson.** 1998. Isolation, cultivation, and characterization of iron- and manganese-reducing bacteria, p. 58–78. *In* R. S. Burlage, R. Atlas, D. A. Stahl, G. Geesey, and G. S. Sayler (ed.), Techniques in microbial ecology. Oxford University Press, New York, N.Y.
26. **Kostka, J. E., A. Roychoudhury, and P. Van Cappellen.** 2002. Rates and controls of anaerobic microbial respiration across spatial and temporal gradients in saltmarsh sediments. Biogeochemistry **60:**49–76.
27. **Kowalchuk, G. A., Z. S. Naoumenko, P. J. L. Derikx, A. Felske, J. R. Stephen, and I. A. Arkhipchenko.** 1999. Molecular analysis of ammonia-oxidizing bacteria of the β subdivision of the class *Proteobacteria* in compost and composted materials. Appl. Environ. Microbiol. **65:**396–403.
28. **Kristensen, E.** 1988. Benthic fauna and biogeochemical processes in marine sediments: microbial activities and fluxes, p. 275–299. *In* T. H. Blackburn and J. Sorensen (ed.), Nitrogen cycling in coastal marine environments, vol. 33. John Wiley & Sons, New York, N.Y.
29. **Kristensen, E., M. H. Jensen, and T. K. Andersen.** 1985. The impact of polychaete (*Nereis virens* Sars.) on nitrification and denitrification in estuarine sediments. J. Exp. Mar. Biol. Ecol. **85:**75–91.
30. **Lee, R. Y., S. B. Joye, B. J. Roberts, and I. Valiela.** 1997. Release of N_2 and N_2O from salt-marsh sediments subject to different land-derived nitrogen loads. Biol. Bull. **193:**292–293.
31. **Nold, S. C., J. Zhou, A. H. Devol, and J. M. Tiedje.** 2000. Pacific Northwest marine sediments contain ammonia-oxidizing bacteria in the β subdivision of the *Proteobacteria*. Appl. Environ. Microbiol. **66:**4532–4535.
32. **Norton, J. M., J. J. Alzerreca, Y. Suwa, and M. G. Klotz.** 2002. Diversity of ammonia monooxygenase operon in autotrophic ammonia-oxidizing bacteria. Arch. Microbiol. **177:**139–149.
33. **Okano, Y., K. R. Hristova, C. M. Leutenegger, L. E. Jackson, R. F. Denison, B. Gebreyesus, D. Lebauer, and K. M. Scow.** 2004. Application of real-time PCR to study effects of ammonium on population size of ammonia-oxidizing bacteria in soil. Appl. Environ. Microbiol. **70:**1008–1016.
34. **Phillips, C. J., E. A. Paul, and J. I. Prosser.** 2000. Quantitative analysis of ammonia oxidizing bacteria using competitive PCR. FEMS Microbiol. Ecol. **32:**167–175.
35. **Prosser, J. I., and T. M. Embley.** 2002. Cultivation-based and molecular approaches to characterisation of terrestrial and aquatic nitrifiers. Antonie Leeuwenhoek **81:**165–179.
36. **Ryther, J. H., and W. M. Dunstan.** 1971. Nitrogen, phosphorus, and eutrophication in the coastal marine environment. Science **171:**1008–1013.
37. **Schmidt, I., and E. Bock.** 1997. Anaerobic ammonia oxidation with nitrogen dioxide by *Nitrosomonas eutropha*. Arch. Microbiol. **167:**106–111.
38. **Sørensen, J.** 1978. Denitrification rates in a marine sediment as measured by the acetylene inhibition technique. Appl. Environ. Microbiol. **36:**139–143.
39. **Stephen, J. R., A. E. McCaig, Z. Smith, J. I. Prosser, and T. M. Embley.** 1996. Molecular diversity of soil and marine 16S rRNA gene sequences related to β-subgroup ammonia-oxidizing bacteria. Appl. Environ. Microbiol. **62:**4147–4154.
40. **Stookey, L. L.** 1970. Ferrozine—a new spectrophotometric reagent for iron. Anal. Chem. **43:**779–781.
41. **Thamdrup, B., H. Fossing, and B. B. Jorgensen.** 1994. Manganese, iron, and sulfur cycling in a coastal marine sediment, Aarhus Bay, Denmark. Geochim. Cosmochim. Acta **58:**5115–5129.
42. **Thompson, S. P., H. W. Paerl, and M. C. Go.** 1995. Seasonal patterns of nitrification and denitrification in a natural and a restored salt marsh. Estuaries **18:**399–408.
43. **Tobias, C. R., I. C. Anderson, E. A. Canuel, and S. A. Macko.** 2001. Nitrogen cycling through a fringing marsh-aquifer ecotone. Mar. Ecol. Prog. Ser. **210:**25–39.
44. **Valiela, I., M. L. Cole, J. McClelland, J. Hauxwell, J. Cebrian, and S. B. Joye.** 2001. Role of salt marshes as part of coastal landscapes, p. 23–38. *In* M. P. Weinstein and D. A. Kreeger (ed.), Concepts and controversies in tidal ecology. Kluwer Academic Publishers, Dordrecht, The Netherlands.
45. **Valiela, I., and J. M. Teal.** 1979. The nitrogen budget of a salt marsh ecosystem. Nature **280:**652–656.
46. **Verity, P. G.** 2002. A decade of change in the Skidaway River estuary. I. Hydrography and nutrients. Estuaries **25:**944–960.
47. **White, D. S., and B. L. Howes.** 1994. Long-term ^{15}N-nitrogen retention in the vegetated sediments of a New England salt marsh. Limnol. Oceanogr. **38:** 1878–1892.
48. **Zehr, J. P., and B. B. Ward.** 2002. Nitrogen cycling in the ocean: new perspectives on processes and paradigms. Appl. Environ. Microbiol. **68:** 1015–1024.